



## Article

# Upcycling Medical Tablet Blister Waste into High-Performance Triboelectric Nanogenerators for Sustainable Energy Harvesting

Vikram Lakshmi Suneetha <sup>1,2</sup>, Velpula Mahesh <sup>1</sup>, Khanapuram Uday Kumar <sup>1</sup> and Rajaboina Rakesh Kumar <sup>1,\*</sup>

<sup>1</sup> Energy Materials and Devices (EMD) Lab, Department of Physics, National Institute of Technology, Warangal 506004, India; suneetha.vikram@gmail.com (V.L.S.); vm22phr2r01@student.nitw.ac.in (V.M.); kanapuram.udaykumar@nitw.ac.in (K.U.K.)

<sup>2</sup> Department of Physics, RVR & JC College of Engineering, Chowdavaram, Guntur 522019, India

\* Correspondence: rakeshr@nitw.ac.in

## Abstract

The increasing accumulation of medical waste, especially discarded pharmaceutical blister packs, poses both environmental risks and missed opportunities for resource recovery. In this work, we demonstrate, for the first time, the direct upcycling of tablet blister waste into a potential frictional layer in triboelectric nanogenerators (TENGs). The polymer structure of blister packs, combined with Silicone rubber as a counter frictional layer, enabled the fabrication of durable TENG devices (TS-TENGs). Systematic electrical testing revealed that the TS-TENG achieved an open-circuit voltage of approximately 300 V, a short-circuit current of about 40  $\mu$ A, and a peak power density of 3.54 W/m<sup>2</sup> at an optimal load resistance of 4 M $\Omega$ . The devices maintained excellent stability over 10,000 mechanical cycles, confirming their durability. Practical demonstrations included powering 240 LEDs, four LED lamps, and portable electronic devices, such as calculators and hygrometers, through capacitor charging. This study shows that not only can tablet blister waste be used as a triboelectric material but it also presents a sustainable method to reduce pharmaceutical waste while advancing self-powered systems. The approach offers a scalable and low-cost means to integrate medical waste management with renewable energy technologies.

**Keywords:** waste to energy; medical waste; tablet blister waste; energy harvesting; triboelectric nanogenerators



Academic Editor: Christian Falconi

Received: 10 September 2025

Revised: 6 November 2025

Accepted: 12 November 2025

Published: 1 December 2025

**Citation:** Suneetha, V.L.; Mahesh, V.; Uday Kumar, K.; Kumar, R.R. Upcycling Medical Tablet Blister Waste into High-Performance Triboelectric Nanogenerators for Sustainable Energy Harvesting. *Nanoenergy Adv.* **2025**, *5*, 19. <https://doi.org/10.3390/nanoenergyadv5040019>

**Copyright:** © 2025 by the authors. Licensee MDPI, Basel, Switzerland. This article is an open access article distributed under the terms and conditions of the Creative Commons Attribution (CC BY) license (<https://creativecommons.org/licenses/by/4.0/>).

## 1. Introduction

Waste generation from various sectors such as agriculture, household, medical, textile, electronic, and automotive sources has been increasing rapidly over the years due to population growth and inadequate recycling methods [1–6]. Most of this waste remains uncollected for recycling or reuse, leading to environmental pollution, ocean contamination, microplastic pollution, health hazards, climate change, and economic costs. Therefore, there is a serious need for new resource utilization technologies, such as recycling, upcycling, and reuse, to be implemented alongside existing technologies. Among the existing methods, waste-to-energy (WTE) technologies such as incineration [7], gasification [8–10], pyrolysis [6,11], and anaerobic digestion [12,13] attracted a lot of attention around the globe and have been implemented. The above method often releases unwanted by-products, as well as carbon dioxide emissions during their reutilization, which leads to risks to the environment. Therefore, there is a need for new technology that has fewer environmental effects and can produce energy. Triboelectric nanogenerator technology is a

renewable technology that uses various waste materials for energy harvesting and sensing applications [14–20]. Triboelectric nanogenerator technology was first introduced by Prof. Z. L. Wang’s group in 2012, and it operates on the principles of contact electrification and electrostatic induction [21]. In TENGs, two different materials with different work functions come into contact and separate repeatedly through mechanical force, which leads to the generation of alternating electrical output in the external circuit [22]. Based on its working principle, this technology can utilize a wide range of materials [23], including polymers [24], oxides [25], semiconductors [26], 2D materials [27], porous materials [28], biomaterials [29], and textiles [30]. In addition to the list above, waste materials are also used in TENGs through upcycling or recycling. So far, in the literature, medical, plastic, household, bio-waste, and electronic waste have been employed in TENG designs for various applications [14–16,31,32].

In the present work, we specifically explore medical waste, particularly tablet blister waste, for TENG design. The tablet blister refers to the discarded plastic–aluminum packaging of pharmaceutical tablets, repurposed as a triboelectric material in the present work. These blisters are typically composed of a polymer (PVC/PET/PVDC) base and aluminum foil, which possess different electron affinities, making them suitable as frictional layers.

Medical tablet blister waste is abundant, low-cost, flexible, and robust. Additionally, we are using plastic as a frictional layer, and an aluminum layer attached to the blister acts as an electrode for the TENG design. These advantages make the tablet blister an ideal candidate for TENG applications. So far, medical waste such as saline bottles, X-ray sheets, ointment tubes, plastic tubing, gloves, masks, and PPE have been explored for TENG design. The detailed literature review of medical waste-based TENGs and their performances is presented in Table 1. To the best of the authors’ knowledge, tablet blisters are being explored for the first time for TENG application.

**Table 1.** Literature review of medical waste-based TENGs.

Sl. No	Medical Waste Type	Opposite Layer	Voltage (V) & Current ( $\mu$ A)	Power Density	Application	Ref.
1	Surgical face mask	Mylar	200 and 48.3	71.16 mW/m <sup>2</sup>	Lighting low-power electronic devices	[33]
2	Laboratory waste (plastic, PET, aluminum, nitrile gloves)	PET	185 and 1.25	81 mW/m <sup>2</sup>	Self-powered human tracking device	[18]
3	Surgical mask (polypropylene)	AL	60 and 3.5	18 mW/m <sup>2</sup>	Self-powered touching sensor	[34]
4	X-ray sheets	Silicone	201 and 62.8	1.39 W/m <sup>2</sup>	Self-powered indicator displays and force sensor	[35]
5	COVID-19 clinical waste (masks and gloves)	Nitrile rubber	50.7 and 4.8	63.9 mW/m <sup>2</sup>	Touch sensor, smart hand sanitizer dispenser	[36]
6	Saline bottle sheets	Silicone	500 and 105	8.78 W/m <sup>2</sup>	Health monitoring and sensing	[37]
7	Medical ointment tubes	Silicone	405 and 82	658 mW/m <sup>2</sup>	Lighting low-power electronic devices	[38]
8	Expired pharmaceutical drugs	PET	561 and 53	1.63 W/m <sup>2</sup>	Lighting low-power electronic devices	[39]
9	Tablet blister waste	Silicone	300 and 40	3.54 W/m <sup>2</sup>	LED lamps, and portable electronic devices continuously.	Present work

In this work, medical waste (tablet blister) is used in TENG with Silicone rubber as the opposite frictional layer. The fabricated TENG exhibited a power density of  $3.54 \text{ W/m}^2$ , and it was utilized for powering LEDs and continuous powering of portable electronic devices with energy management circuits.

## 2. Materials and Methods

Medical waste (tablet blisters) is collected from the local medical clinic, and a photograph of the selected tablet blister is shown in Figure 1a. We chose this particular design because of its flat unused area, which is ideal for the triboelectric frictional layer compared to other designs. In other tablet designs, it is difficult to have a large unused area. The present TS-TENG prototype was designed at a centimeter scale to suit ambient, user-actuated energy harvesting, such as hand tapping or foot pressing. Figure 1b shows the schematic of the TENG device in VCS mode, in which the tablet-insulating surface acts as one fixed frictional layer, and different opposite layers, such as Kapton, Polyethylene Terephthalate (PET), Polymethyl methacrylate (PMMA), Fluorinated Ethylene Propylene (FEP), Polytetrafluoroethylene (PTFE) and Silicone rubber, were tested. We have cut the selected blue color region from the tablet blister to obtain a flat sheet of size ( $3.8 \times 2.5 \text{ cm}^2$ ) and attached it to cardboard using double-sided adhesive tape, as shown in Figure 1c. The plastic surface faces upward, with the conducting aluminum behind it. The bottom aluminum serves as one electrode, and the plastic surface functions as the frictional layer. Figure 1c displays the Silicone rubber frictional layer attached to the supporting cardboard with aluminum and conducting carbon tape. Two supporting cardboard pieces with their frictional layers are placed one over the other using a sponge spacer to assemble the final TENG device. The sponge spacer creates a gap of about 1 cm between the frictional layers. Two aluminum electrodes are connected to the measuring devices with connecting wires. We prepared a total of six TENG devices, each using a fixed tablet blister plastic layer paired with different opposite frictional layers: PET, Kapton, PMMA, PTFE, FEP, and Silicone rubber. The tablet blister-based TENG (TS-TENG) devices are tested through repeated hand tapping at a frequency of 4–5 Hz under ambient conditions. The TENG device's open-circuit voltage ( $V_{oc}$ ) and short-circuit current ( $I_{sc}$ ) were measured using a digital storage oscilloscope (GW-Instek, GDS-1102B, New Taipei City, Taiwan) and a current preamplifier (SR 570, SRS instruments, Sunnyvale, CA, USA). A decade resistance box (Nvis 705, Indore, India) was used to perform the load characteristics of the TENG. An in-house developed linear motor was used for testing TS-TENG for a large number of test cycles.

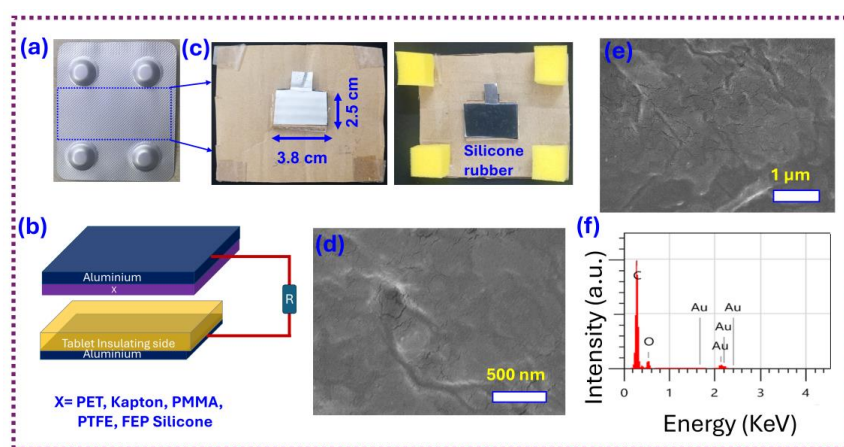


**Figure 1.** (a) Photograph of the tablet blister, (b) schematic of the TENG device in VCS mode, (c) photographs of the frictional layers tablet blister and Silicone rubber attached to supporting cardboard sheets, (d,e) SEM images of the tablet blister insulating surface at different magnifications, (f) EDX spectrum of the blister insulating surface.

### 3. Results

#### 3.1. Material Characterization

The morphology of the insulating side of the tablet blister is examined using a scanning electron microscope (SEM, JEOL-JSM-IT800, Tokyo, Japan), and the surface features are shown in Figure 1d,e. SEM images reveal that the surface has a rough texture throughout the substrate, which helps increase the effective contact area during TENG operation through contact electrification. Compositional analysis was performed on the entire surface, and the EDX results are presented in Figure 1f. EDX results confirm the presence of carbon (C), oxygen (O), and gold (Au). The tablet blister is made of a polymer whose composition includes carbon and oxygen, and the Au peaks originate from the gold coating applied to it. Furthermore, we have performed XRD and FT-IR spectra analysis, and it is difficult to identify the exact material of the tablet blister's non-conducting surface material. The spectra are presented in the Supplementary Materials Figure S1.

#### 3.2. Electrical Characterization of the TENG

The bio-mechanical energy harvesting capability of the prepared tablet blister—TENGs devices were tested under repeated hand tapping with different opposing frictional layers, and the results are presented in Figure 2a. It is clear that the tablet blister surface acts like a triboelectric-positive material; when paired with another triboelectric-positive material (PET, PMMA), it produces low output, and when paired with a triboelectric-negative material (FEP, Silicone rubber), it generates high electrical output. The highest energy conversion occurred for the tablet blister–Silicone rubber triboelectric pair, with an open-circuit voltage and short-circuit current of approximately 300 V and 40  $\mu\text{A}$ , respectively. To establish reproducibility, we fabricated six independent replicas of the blister–Silicone TENGs and measured each device response under identical conditions. All quantitative response plots are presented with error bars in the Supplementary Materials Figure S2. The results from the replicas are consistent in trend and magnitude, confirming that the observed behavior is statistically robust. In the next section, a detailed electrical characterization of the tablet blister–Silicone rubber TENG (TS-TENG) is presented.

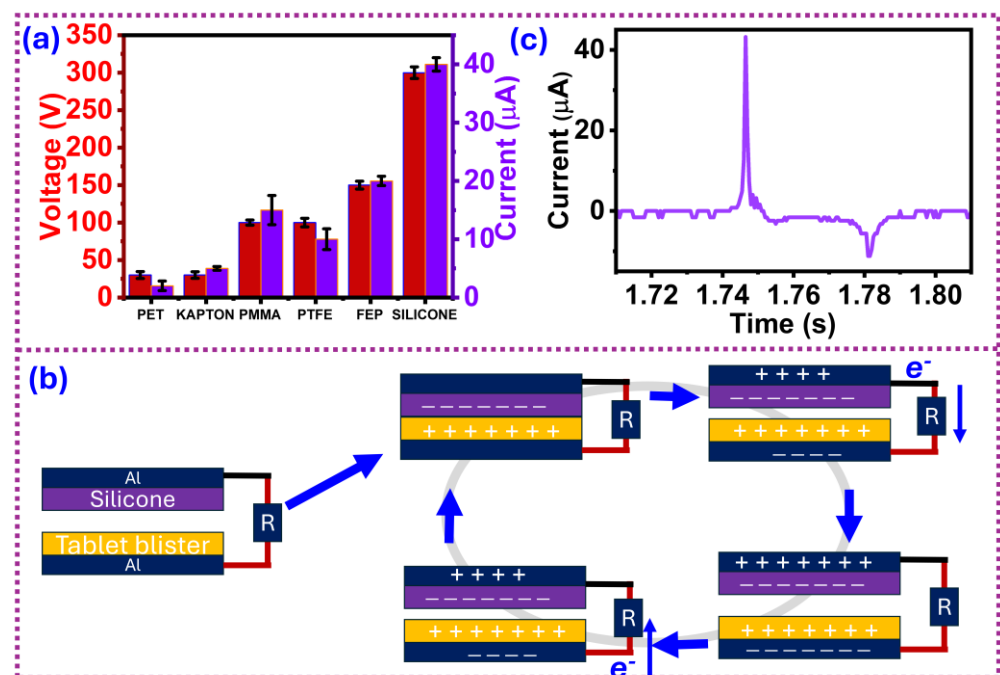


**Figure 2.** (a) Tablet TENG devices electrical output responses, (b) current generation mechanism of tablet blister–Silicone rubber TENG, (c) short-circuit current response of TENG in one cycle.

The current generation mechanism of the TS-TENG is illustrated in Figure 2b. Initially, when both frictional layers are well-separated, there is no current flow in the external circuit. When a hand-tapping force is applied to the TENG, both frictional layers come into contact, and due to differences in their electron affinities, they exchange charges. The Silicone rubber film gains electrons and becomes negatively charged, while the tablet surface loses electrons and becomes positively charged. This charge exchange leads to balancing their Fermi levels. Upon the release of the applied force, the frictional layers separate, and charges on both layers develop a potential difference, resulting in current flow in the external circuit. When they are completely separated, equilibrium is established, and no current is observed. When the hand-tapping force is applied again, it disturbs the equilibrium state, causing the current to flow in the reverse direction. This cycle of contacting and separating the frictional layers results in an alternating current (AC) in the external circuit, and one such response is presented in Figure 2c.

The detailed electrical characterization of TS-TENG is presented in Figure 3. Initially, TS-TENG's open-circuit voltage and short-circuit current are recorded under the switching polarity test configuration [40,41]. The results of the switching polarity test are shown in Figure 3a,b, and it is clear that output responses reverse upon reversal of connections to the measuring instrument. This confirms that the electrical output is generated from the TENG device and not from noise or artifacts. The open-circuit voltage and short-circuit current consistently hovered around  $\sim 300$  V and  $40 \mu\text{A}$ , respectively. This observation clearly confirms the repeatability of the TENG output and consistent tapping force.

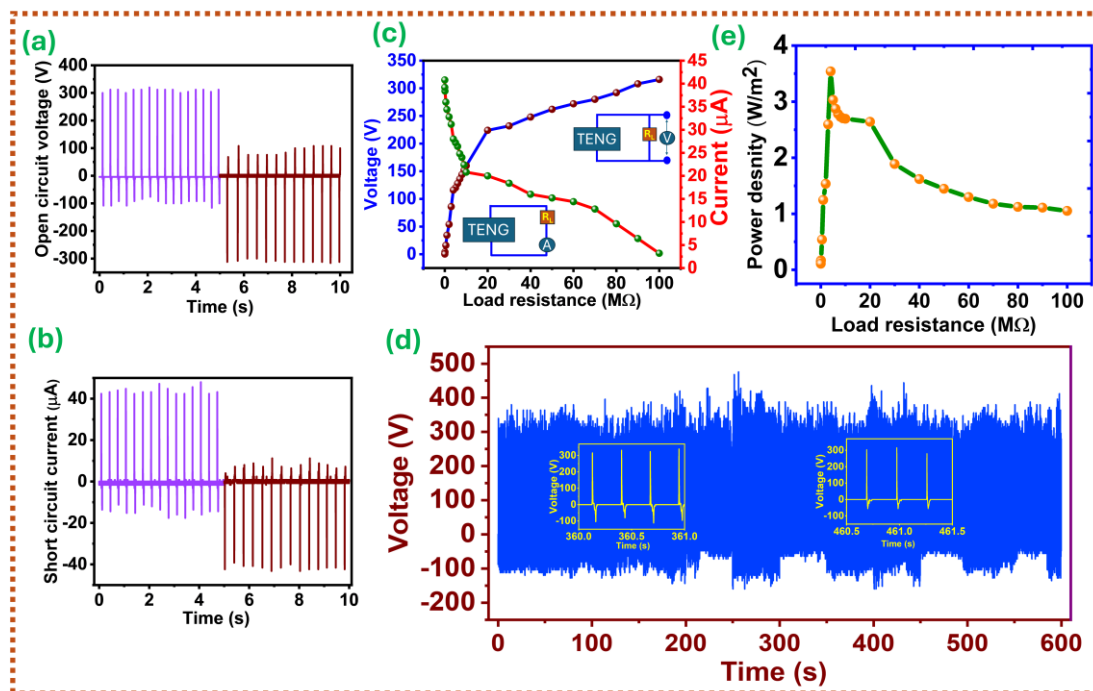


**Figure 3.** TS-TENG switching polarity test results (a) voltage, (b) current, TS-TENG (c) load characteristics, (d) power density variation with load resistance, (e) long-term stability of TS-TENG against 2000 cycles of hand tapping.

To find out the instantaneous power density of the TS-TENG, the electrical responses of the TS-TENG were measured under different load resistance conditions. At each load resistance value, both voltage and current outputs were recorded for about 20 cycles, and the average values were taken. The average output voltage and current at different load resistances are shown in Figure 3c.

The output voltage increased with load resistance and saturated at higher resistances. The output voltage at higher resistance is close to the open-circuit voltage, and conversely, current output decreases with load resistance due to ohmic losses. The observed load characteristics are well-aligned with all the reported literature on TENGs [42,43]. The instantaneous power density ( $P_d$ ) was calculated using load characteristics data and the following formula  $P_d = \frac{V^2}{(R_L A)}$ , where  $A$  is the active area of the TENG. Figure 3e shows the power density variation in TS-TENG with load. Initially, it increases with load and reaches a maximum value of 3.54 W/m<sup>2</sup> at 4 MΩ, then decreases. The observed behavior is well-aligned with the reported literature on TENGs. Table 1 shows the performance of various medical waste-based TENG devices reported so far in the literature. It is clear that the reported performance (current, voltage, and power density) of present TENGs is comparable to the reported values. The present configuration can be easily scaled up by tiling larger or multi-cavity blister sheets. Such modular scaling increases the effective area without altering the surface properties, thereby proportionally enhancing power output. Moreover, connecting multiple blister units in parallel can further increase current for practical energy storage and powering applications.

Finally, the long-term stability of the TENG was tested using an in-house designed tapping machine for 50 min at a frequency of 4–5 Hz, which corresponds to more than 10,000 cycles under ambient conditions (Supplementary Materials Figure S3). Afterward, the device was tested for an additional 2000 hand-tapping cycles. The response to these 2000 hand-tapping cycles is shown in Figure 3d, and it is clear that the device consistently reproduces the same output levels. However, minor changes in the output are due to slight variations in the hand-tapping force. A magnified view of a few cycles from the stability test is shown in the inset of Figure 3d. After the stability test, we did not observe any physical degradation of either of the frictional layers, which further confirms the mechanical robustness of the fabricated TS-TENG.

### 3.3. Applications of TS-TENGs

The practical applications of TS-TENG are shown in Figure 4. Initially, TS-TENG output was rectified using a bridge rectifier, and the pulsed DC output was used to power LEDs, LED lamps, and charge capacitors, which in turn powered portable electronic devices. Figure 4a,b shows photographs of the 240 LEDs in OFF and ON states, briefly powered by TS-TENG for each hand tapping, with the real-time demonstration available in Supplementary Materials Video S1. Similarly, TS-TENG was able to power four LED lamps (two 9 W and two 3 W) briefly for each hand tapping, with the real-time demonstration shown in Supplementary Materials Video S2.

To power portable electronic devices, a 10 μF capacitor charged to approximately 1.5 V is used for powering digital calculators and hygrometers. The charging and discharging profile of the capacitor during powering is shown in Figure 4e,f. Real-time photographs of the calculator and hygrometer in operation are shown in the inset of Figure 4e,f. To power portable electronic devices continuously, we utilized a power-management circuit, as shown in Figure 4g. The switched-capacitor-converter circuit was adopted from the literature due to its simple design and cost-effectiveness [44,45]. In this setup, energy stored in the capacitor is connected in series and discharges in parallel mode. It took 53 s of continuous hand tapping on the TENG to turn on the digital watch initially, and it remained on as long as hand tapping continued. The real-time demonstration of continuous powering of the digital watch is shown in Supplementary Materials, Video S3. These results confirm that the upcycled tablet blister waste not only provides an eco-friendly alternative material but also enables sustainable energy solutions for self-powered systems.

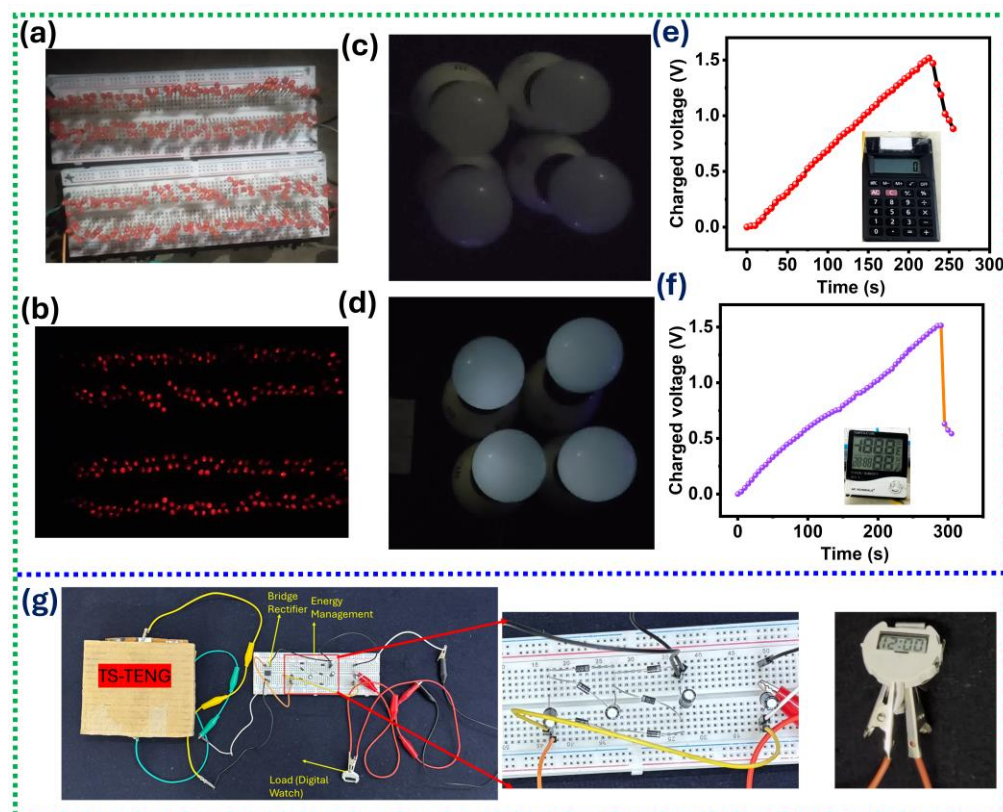


**Figure 4.** (a,b) Photographs of the 240 LEDs in OFF and ON state, (c,d) photographs of the four LED lamps in OFF and ON state, (e,f) charging and discharging profiles of capacitor in powering calculator and hygrometer (inset photographs of devices in ON condition), (g) integration of TENG with energy management circuit for continuous powering of digital watch.

#### 4. Conclusions

In conclusion, the present work introduces a sustainable approach for converting pharmaceutical tablet blister waste into high-performance triboelectric nanogenerators for mechanical energy harvesting. The unique polymer–aluminum structure of blister packs, paired with Silicone rubber, enabled efficient energy harvesting through contact electrification, producing an open-circuit voltage of  $\sim 300$  V, a short-circuit current of  $\sim 40$   $\mu$ A, and a peak power density of  $3.54$  W/m<sup>2</sup>. Electrical characterization confirmed stable and repeatable performance, while long-term testing demonstrated durability over more than 10,000 mechanical cycles. Practical demonstrations, such as powering 240 LEDs, four LED lamps, calculators, and hygrometers, as well as continuously operating a digital watch through an integrated power-management circuit, underscore the real-world potential of the developed TENGs. These results establish medical packaging waste as a robust and cost-effective triboelectric material, addressing both environmental concerns of plastic–aluminum waste and the demand for clean, decentralized energy solutions. By integrating waste management with renewable energy harvesting, this strategy advances circular economy practices and provides a scalable pathway for upcycling diverse medical wastes into functional energy devices.

**Supplementary Materials:** The following supporting information can be downloaded at <https://www.mdpi.com/article/10.3390/nanoenergyadv5040019/s1>, Video S1: Powering LEDs with TS-TENG device; Video S2: Powering LED lamps with TS-TENG device; Video S3: Continuous operation of a digital watch with power-management circuit; Figure S1: Tablet blister XRD and FTIR spectra; Figure S2: Device-to-device reproducibility of the open-circuit voltage (Voc) for six independent

tablet-blister/Silicone-rubber TENGs (TS-TENG); Figure S3: TS-TENG responses with machine tapping for more than 10,000 cycles.

**Author Contributions:** Conceptualization, R.R.K.; methodology, R.R.K. and V.L.S.; validation, V.L.S. and K.U.K.; formal analysis R.R.K., K.U.K. and V.L.S.; investigation, V.L.S.; resources, V.M. and V.L.S.; writing—original draft preparation, V.L.S. and R.R.K.; writing—review and editing, K.U.K., R.R.K. and V.L.S.; visualization, V.L.S. and V.M.; supervision, R.R.K.; project administration, K.U.K. and R.R.K. All authors have read and agreed to the published version of the manuscript.

**Funding:** This research received no external funding.

**Data Availability Statement:** The original contributions presented in this study are included in the article and Supplementary Materials. Further inquiries can be directed to the corresponding author.

**Acknowledgments:** The authors would like to thank the Department of Physics and Centre for Research and Instrument Facility (CRIF), NIT Warangal, for providing their research facilities.

**Conflicts of Interest:** The authors declare no conflict of interest.

## References

1. Moustakas, K.; Loizidou, M.; Klemes, J.; Varbanov, P.; Hao, J.L. New Developments in Sustainable Waste-to-Energy Systems. *Energy* **2023**, *284*, 129270. [[CrossRef](#)]
2. Themelis, N.J. An Overview of the Global Waste-to-Energy Industry. *Waste Manag. World* **2003**, 40–48.
3. Shahabuddin, M.; Uddin, M.N.; Chowdhury, J.I.; Ahmed, S.F.; Uddin, M.N.; Mofijur, M.; Uddin, M.A. A Review of the Recent Development, Challenges, and Opportunities of Electronic Waste (e-Waste). *Int. J. Environ. Sci. Technol.* **2023**, *20*, 4513–4520. [[CrossRef](#)]
4. Foster, W.; Azimov, U.; Gauthier-Maradei, P.; Molano, L.C.; Combrinck, M.; Munoz, J.; Esteves, J.J.; Patino, L. Waste-to-Energy Conversion Technologies in the UK: Processes and Barriers—A Review. *Renew. Sustain. Energy Rev.* **2021**, *135*, 110226. [[CrossRef](#)]
5. Krishnan, S.; Zulkapli, N.S.; Kamyab, H.; Taib, S.M.; Din, M.F.B.M.; Majid, Z.A.; Chaiprapat, S.; Kenzo, I.; Ichikawa, Y.; Nasrullah, M.; et al. Current Technologies for Recovery of Metals from Industrial Wastes: An Overview. *Env. Technol. Innov.* **2021**, *22*, 101525. [[CrossRef](#)]
6. Anuar Sharuddin, S.D.; Abnisa, F.; Wan Daud, W.M.A.; Aroua, M.K. A Review on Pyrolysis of Plastic Wastes. *Energy Convers. Manag.* **2016**, *115*, 308–326. [[CrossRef](#)]
7. Makarichi, L.; Jutidamrongphan, W.; Techato, K. The Evolution of Waste-to-Energy Incineration: A Review. *Renew. Sustain. Energy Rev.* **2018**, *91*, 812–821. [[CrossRef](#)]
8. Lopez, G.; Artetxe, M.; Amutio, M.; Alvarez, J.; Bilbao, J.; Olazar, M. Recent Advances in the Gasification of Waste Plastics. A Critical Overview. *Renew. Sustain. Energy Rev.* **2018**, *82*, 576–596. [[CrossRef](#)]
9. Zhou, H.; Sun, S.; Xu, Y.; Zhang, Y.; Yi, S.; Wu, C. Upcycling Municipal Solid Waste to Sustainable Hydrogen via Two-Stage Gasification-Reforming. *J. Energy Chem.* **2024**, *96*, 611–624. [[CrossRef](#)]
10. Cudjoe, D.; Wang, H. Plasma Gasification versus Incineration of Plastic Waste: Energy, Economic and Environmental Analysis. *Fuel Process. Technol.* **2022**, *237*, 107470. [[CrossRef](#)]
11. Armenise, S.; SyieLuing, W.; Ramírez-Velásquez, J.M.; Launay, F.; Wuebben, D.; Ngadi, N.; Rams, J.; Muñoz, M. Plastic Waste Recycling via Pyrolysis: A Bibliometric Survey and Literature Review. *J. Anal. Appl. Pyrolysis* **2021**, *158*, 105265. [[CrossRef](#)]
12. Emebu, S.; Pecha, J.; Janáčová, D. Review on Anaerobic Digestion Models: Model Classification & Elaboration of Process Phenomena. *Renew. Sustain. Energy Rev.* **2022**, *160*, 112288. [[CrossRef](#)]
13. Zamri, M.F.M.A.; Hasmady, S.; Akhbar, A.; Ideris, F.; Shamsuddin, A.H.; Mofijur, M.; Fattah, I.M.R.; Mahlia, T.M.I. A Comprehensive Review on Anaerobic Digestion of Organic Fraction of Municipal Solid Waste. *Renew. Sustain. Energy Rev.* **2021**, *137*, 110637. [[CrossRef](#)]
14. Kumar, K.U.; Hajra, S.; Mohana Rani, G.; Panda, S.; Umaphathi, R.; Venkateswarlu, S.; Kim, H.J.; Mishra, Y.K.; Kumar, R.R. Revolutionizing Waste-to-Energy: Harnessing the Power of Triboelectric Nanogenerators. *Adv. Compos. Hybrid Mater.* **2024**, *7*, 91. [[CrossRef](#)]
15. Ahmed, A.A.; Qahtan, T.F.; Owolabi, T.O.; Agunloye, A.O.; Rashid, M.; Mohamed Ali, M.S. Waste to Sustainable Energy Based on TENG Technology: A Comprehensive Review. *J. Clean. Prod.* **2024**, *448*, 141354. [[CrossRef](#)]
16. Basith, S.A.; Khandelwal, G.; Mulvihill, D.M.; Chandrasekhar, A. Upcycling of Waste Materials for the Development of Triboelectric Nanogenerators and Self-Powered Applications. *Adv. Funct. Mater.* **2024**, *34*, 2408708. [[CrossRef](#)]

17. Sahu, M.; Hajra, S.; Jadhav, S.; Panigrahi, B.K.; Dubal, D.; Kim, H.J. Bio-Waste Composites for Cost-Effective Self-Powered Breathing Patterns Monitoring: An Insight into Energy Harvesting and Storage Properties. *Sustain. Mater. Technol.* **2022**, *32*, e00396. [[CrossRef](#)]
18. Sahu, M.; Hajra, S.; Kim, H.G.; Rubahn, H.G.; Kumar Mishra, Y.; Kim, H.J. Additive Manufacturing-Based Recycling of Laboratory Waste into Energy Harvesting Device for Self-Powered Applications. *Nano Energy* **2021**, *88*, 106255. [[CrossRef](#)]
19. Sahu, M.; Hajra, S.; Panda, S.; Rajaitha, M.; Panigrahi, B.K.; Rubahn, H.G.; Mishra, Y.K.; Kim, H.J. Waste Textiles as the Versatile Triboelectric Energy-Harvesting Platform for Self-Powered Applications in Sports and Athletics. *Nano Energy* **2022**, *97*, 107208. [[CrossRef](#)]
20. Panda, S.; Hajra, S.; Kim, H.-G.; Achary, P.G.R.; Pakawanit, P.; Yang, Y.; Mishra, Y.K.; Kim, H.J. Sustainable Solutions for Oral Health Monitoring: Biowaste-Derived Triboelectric Nanogenerator. *ACS Appl. Mater. Interfaces* **2023**, *15*, 36096–36106. [[CrossRef](#)]
21. Fan, F.R.; Tian, Z.Q.; Wang, Z.L. Flexible Triboelectric Generator. *Nano Energy* **2012**, *1*, 328–334. [[CrossRef](#)]
22. Wu, C.; Wang, A.C.; Ding, W.; Guo, H.; Wang, Z.L. Triboelectric Nanogenerator: A Foundation of the Energy for the New Era. *Adv. Energy Mater.* **2019**, *9*, 1802906. [[CrossRef](#)]
23. Zhang, R.; Olin, H. Material Choices for Triboelectric Nanogenerators: A Critical Review. *EcoMat* **2020**, *2*, e12062. [[CrossRef](#)]
24. Shanbedi, M.; Ardebili, H.; Karim, A. Polymer-Based Triboelectric Nanogenerators: Materials, Characterization, and Applications. *Prog. Polym. Sci.* **2023**, *144*, 101723. [[CrossRef](#)]
25. Potu, S.; Kulandaivel, A.; Gollapelli, B.; Khanapuram, U.K.; Rajaboina, R.K. Oxide Based Triboelectric Nanogenerators: Recent Advances and Future Prospects in Energy Harvesting. *Mater. Sci. Eng. R Rep.* **2024**, *161*, 100866. [[CrossRef](#)]
26. Shi, X.; Wang, W.; Wang, J.; Li, J.; Chen, H. Semiconductor-Based Direct Current Triboelectric Nanogenerators and Its Application. *J. Semicond.* **2024**, *45*, 121701. [[CrossRef](#)]
27. Rajaboina, R.K.; Khanapuram, U.K.; Kulandaivel, A. 2D Layered Materials Based Triboelectric Self-Powered Sensors. *Adv. Sens. Res.* **2024**, *3*, 2400045. [[CrossRef](#)]
28. Rajaboina, R.K.; Khanapuram, U.K.; Vivekananthan, V.; Khandelwal, G.; Potu, S.; Babu, A.; Madathil, N.; Velpula, M.; Kodali, P. Crystalline Porous Material-Based Nanogenerators: Recent Progress, Applications, Challenges, and Opportunities. *Small* **2024**, *20*, 2306209. [[CrossRef](#)]
29. Song, K.Y.; Kim, S.W.; Nguyen, D.C.; Park, J.Y.; Luu, T.T.; Choi, D.; Baik, J.M.; An, S. Recent Progress on Nature-Derived Biomaterials for Eco-Friendly Triboelectric Nanogenerators. *EcoMat* **2023**, *5*, e12357. [[CrossRef](#)]
30. Paosangthong, W.; Torah, R.; Beeby, S. Recent Progress on Textile-Based Triboelectric Nanogenerators. *Nano Energy* **2019**, *55*, 401–423. [[CrossRef](#)]
31. Vikram, L.S.; Potu, S.; Kasireddi, A.K.D.P.; Khanapuram, U.K.; Divi, H.; Rajaboina, R.K. Biowaste Sea Shells-Based Triboelectric Nanogenerator: Sustainable Approach for Efficient Mechanical Energy Harvesting. *Energy Technol.* **2025**, *13*, 2401333. [[CrossRef](#)]
32. Suneetha, V.L.; Mahesh, V.; Supraja, P.; Navaneeth, M.; Uday Kumar, K.; Rakesh Kumar, R. Facile and Robust High-Performance Triboelectric Nanogenerator Based on Electronic Waste for Self-Powered Electronics. *Energy Technol.* **2025**, *13*, 2401387. [[CrossRef](#)]
33. Varghese, H.; Chandran, A. Triboelectric Nanogenerator from Used Surgical Face Mask and Waste Mylar Materials Aiding the Circular Economy. *ACS Appl. Mater. Interfaces* **2021**, *13*, 51132–51140. [[CrossRef](#)]
34. Shen, D.; Xiao, M.; Zhao, X.; Xiao, Y.; Duley, W.W.; Zhou, Y.N. Multifunctional Self-Powered Electronics Based on a Reusable Low-Cost Polypropylene Fabric Triboelectric Nanogenerator. *ACS Appl. Mater. Interfaces* **2021**, *13*, 34266–34273. [[CrossRef](#)]
35. Navaneeth, M.; Potu, S.; Babu, A.; Rajaboina, R.K.; Kumar, U.; Divi, H.; Kodali, P. A Medical Waste X-Ray Film Based Triboelectric Nanogenerator for Self-Powered Devices, Sensors, and Smart Buildings. *Environ. Sci. Adv.* **2023**, *2*, 848–860. [[CrossRef](#)]
36. Basith, S.A.; Chandrasekhar, A. COVID-19 Clinical Waste Reuse: A Triboelectric Touch Sensor for IoT-Cloud Supported Smart Hand Sanitizer Dispenser. *Nano Energy* **2023**, *108*, 108183. [[CrossRef](#)] [[PubMed](#)]
37. Navaneeth, M.; Potu, S.; Babu, A.; Lakshakoti, B.; Rajaboina, R.K.; Kumar, K.U.; Divi, H.; Kodali, P.; Balaji, K. Transforming Medical Plastic Waste into High-Performance Triboelectric Nanogenerators for Sustainable Energy, Health Monitoring, and Sensing Applications. *ACS Sustain. Chem. Eng.* **2023**, *11*, 12145–12154. [[CrossRef](#)]
38. Lakshmi Suneetha, V.; Supraja, P.; Uday Kumar, K.; Rakesh Kumar, R. Sustainable Energy Harvesting from Medical Waste: Utilizing Discarded Ointment Tubes in Triboelectric Nanogenerators. *Mater. Lett.* **2024**, *377*, 137350. [[CrossRef](#)]
39. Chougale, M.Y.; Saqib, Q.M.; Khan, M.U.; Shaikat, R.A.; Kim, J.; Dubal, D.; Bae, J. Expired Pharmaceutical Drugs as Tribopositive Material for Triboelectric Nanogenerator. *Adv. Sustain. Syst.* **2021**, *5*, 2100205. [[CrossRef](#)]
40. Yang, R.; Qin, Y.; Li, C.; Dai, L.; Wang, Z.L. Characteristics of Output Voltage and Current of Integrated Nanogenerators. *Appl. Phys. Lett.* **2009**, *94*, 92–95. [[CrossRef](#)]
41. Vivekananthan, V.; Chandrasekhar, A.; Alluri, N.R.; Purusothaman, Y.; Kim, S.J. A Highly Reliable, Impervious and Sustainable Triboelectric Nanogenerator as a Zero-Power Consuming Active Pressure Sensor. *Nanoscale Adv.* **2020**, *2*, 746–754. [[CrossRef](#)] [[PubMed](#)]
42. Behera, S.A.; Kim, H.G.; Jang, I.R.; Hajra, S.; Panda, S.; Vittayakorn, N.; Kim, H.J.; Achary, P.G.R. Triboelectric Nanogenerator for Self-Powered Traffic Monitoring. *Mater. Sci. Eng. B* **2024**, *303*, 117277. [[CrossRef](#)]

43. Behera, S.A.; Kaja, K.R.; Hajra, S.; Panda, S.; Sahu, A.K.; Belal, M.A.; Alagarsamy, P.; Vivekananthan, V.; Kim, H.J.; Achary, P.G.R. Self-Powered Wind Flow Monitoring Unit Using Lead-Free Composites-Based Triboelectric Nanogenerator. *ACS Appl. Energy Mater.* **2025**, *8*, 6688–6698. [[CrossRef](#)]
44. Liu, W.; Wang, Z.; Wang, G.; Zeng, Q.; He, W.; Liu, L.; Wang, X.; Xi, Y.; Guo, H.; Hu, C.; et al. Switched-Capacitor-Convertors Based on Fractal Design for Output Power Management of Triboelectric Nanogenerator. *Nat. Commun.* **2020**, *11*, 1883. [[CrossRef](#)] [[PubMed](#)]
45. Mishra, S.; Supraja, P.; Haranath, D.; Kumar, R.R.; Pola, S. Effect of Surface and Contact Points Modification on the Output Performance of Triboelectric Nanogenerator. *Nano Energy* **2022**, *104*, 107964. [[CrossRef](#)]

**Disclaimer/Publisher's Note:** The statements, opinions and data contained in all publications are solely those of the individual author(s) and contributor(s) and not of MDPI and/or the editor(s). MDPI and/or the editor(s) disclaim responsibility for any injury to people or property resulting from any ideas, methods, instructions or products referred to in the content.